Low-Temperature Growth of Inverted Hexagonal ZnS/CdS Quantum Dots: Functional and Luminescence Properties

HITANSHU KUMAR,[1] P.B. BARMAN,[1] and RAGINI RAJ SINGH[1,2,3]

1.—Department of Physics and Materials Science, Jaypee University of Information Technology, Waknaghat, Solan 173234, HP, India. 2.—e-mail: raginirajsingh@gmail.com. 3.—e-mail: ragini.rajsingh@juit.ac.in

A novel low-temperature wet chemical method is proposed for direct growth of type-I inverted hexagonal ZnS/CdS quantum dots (QD). 2-Mercaptoethanol (2-ME) was used as a capping agent for confinement by passivation, and also helped to prevent agglomeration of the QD. The band gap calculated from optical absorption spectra was 2.63 eV for the smallest core/shell QD. Absorption edge onset and results from transmission electron microscopy revealed formation of inverted core/shell QD. X-ray diffraction studies revealed the ZnS/CdS had a stable hexagonal crystal structure at low temperature. The average diameter of the core/shell QD was 4.2 nm. Tunable luminescence with substantial tunability was revealed by study of the photoluminescence of the inverted ZnS/CdS quantum dots. Surface passivation of ZnS/CdS QD by 2-ME was confirmed by Fourier-transform infrared spectroscopy.

Key words: Quantum dots, inverted core/shell structures, electron microscopy, luminescence, FTIR

INTRODUCTION

Inverted quantum dots (QD) synthesized by wet chemical methods are being actively investigated because of their adjustable optical and electronic properties. QD are extremely valuable in a variety of applications, for example light-emitting diodes, photovoltaic devices, lasers, and biological labeling, among others.[1,2] The optical and structural properties of these materials can be modified by controlling the size of the QD.[3] In general, for all types of core/shell QD (e.g. CdS/ZnS), the shell increases quantum yield by passivating the surface trap states, by providing a physical barrier between the optically active core and the surrounding medium. The shell also provides protection against environmental and photo-oxidative degradation, and is another means of modification of the QD by making the core/shell less sensitive to perturbations. Strict control of size and shape results in QD with narrow FWHM (full width at half maximum) and hence high fluorescence quantum yield. Good monodispersity is also achieved for core/shell QD.

These effects are fundamental to use of core/shell QD in such applications as biological labeling and in light-emitting devices, which depend on the emission properties of the QD. In inverted core/shell structures a wide-band-gap semiconductor core is coated with a shell of a narrower-band-gap material. The core and shell enable the emission wavelength to be manipulated over a wider range of wavelengths than for either individual semiconductor. It is possible to control the functionality of these "inverted" QD by direct control of the distribution of electron and hole wave functions and the electron–hole (e–h) overlap integral by increasing the thickness of the nanocrystalline (NC) shell for a fixed core size.[4]

In this study we investigated the optimum synthetic conditions, photoluminescence (PL) emission behavior, and surface modification of inverted hexagonal ZnS/CdS QD capped by the thiol 2-mercaptoethanol (2-ME) at low temperature. The size of the core was fixed and the shell thicknesses varied by controlling the size of the shell by use of the capping agent. Surface modification of a wide-band-gap (ZnS) material surrounded by a narrow-band-gap (CdS) material can be used to modify the orientation

of charges and the reactivity of the materials. This results in enhancement of PL emission intensity because of localization of $e–h$ pairs.[5–7] This implies that the wave functions of electrons and holes may be spatially separated in the core and shell, reducing the probability of non-radiative decay of surface states and trap sites.[8] This behavior of ZnS/CdS is attractive because of unique localization of $e–h$ pairs compared with other core/shell QD. Several different combinations of core/shell QD, for example CdSe/ZnS, CdS/ZnS, ZnO/ZnS, ZnSe/ZnS, CdSe/CdS, CdS/PbS, and ZnSe/CdS have previously been studied.[9,10] The highlight and novelty of our work is formation and analysis of the structural and optical properties and surface nature of luminescent wurtzite ZnS/CdS core/shell QD synthesized at low temperature ($35 \pm 1°C$). Characterization was performed after each stage of the growth of CdS, ZnS, and ZnS/CdS. A few other workers have also synthesized ZnS/CdS by use of different methods, for example chemical methods in an air atmosphere, and many other authors have also reported on ZnS/CdS QD but used other methods of synthesis and obtained particles with cubic structures. Very few authors have reported wurtzite ZnS/CdS QD, and their methods were different or they used physical synthesis at high temperatures.[11–15] Some of the reports are theoretical presentations. Inverted hexagonal ZnS/CdS QD will be useful when enhancement and tuning of optical properties is needed with eco-friendly material and biocompatible properties.[16] A possible mechanism of growth of these promising QD is proposed in this report.

EXPERIMENTAL

Synthesis of ZnS/CdS QD

ZnS/CdS core/shell structures were synthesized by the seed growth method. To synthesize the desired QD we prepared ZnS QD as seeds by the solution growth method at $35 \pm 1°C$ with a fixed amount of 2-mercaptoethanol. This method of preparation usually uses a complexing agent to control the release of metal ions (Zn^{2+}) and sulfur ions (S^{2-}) to ensure a controlled homogeneous reaction. The reaction matrix used in this study consisted of AR grade $CdCl_2$, NH_4Cl, and thiourea, in 1:1.5:3 molar ratio, for CdS, and AR grade $ZnSO_4$, $(NH_4)_2SO_4$, and thiourea, in 1:1.5:1.5 molar ratio, for ZnS. First we prepared the ZnS seed QD; for this the reaction matrix was prepared in two parts. The initial solutions were prepared from anhydrous zinc sulfate ($ZnSO_4$) and ammonium sulfate ($(NH_4)_2SO_4$) in 50 ml water. Ammonia (NH_3) was used as complexing agent until formation of the clear metal complexes and the pH was kept at 7. Thiourea, $CS(NH_2)_2$, was then added as the source of sulfur in the prepared solution. Immediately 2 ml 5% 2-ME solution was added as a capping agent to control the particle size of the QD, and the mixture was stirred continuously for 5 h. After synthesis the ZnS-containing sample was centrifuged

(3500 rpm, 20 min) and the product was washed several times with distilled water and dried.

To synthesize ZnS/CdS core/shell QD, a CdS shell layer was grown on the ZnS core nanocrystals. The method of CdS shell formation was same as for the seed ZnS QD for the source of cadmium, which was cadmium chloride ($CdCl_2$) and the respective complexing agent, ammonium chloride (NH_4Cl), instead of zinc sulfate ($ZnSO_4$) and ammonium sulfate ($(NH_4)_2SO_4$). As an additional step for synthesis of the core/shell structures 0.1 g of the prepared ZnS QD was added just before addition of the thiourea. The required amount of 2-ME (1 ml, 2 ml, and 4 ml of 5% 2-ME solution) was then added to the solution for capping and to obtain a series of inverted hexagonal ZnS/CdS core/shell structures with different shell thickness and size. This wet chemical method for synthesis of ZnS/CdS core/shell structures is shown schematically in Fig. 1. This process is a very efficient in terms of reproducibility and preparation time and enables preparation of QD with well controlled size, shape, and monodispersity (by changing such experimental conditions as concentration, temperature, and pH of the precursor solutions).

Among the different methods used to grow nanocrystals, solution growth at low temperatures is widely used because of its versatility and simplicity. After many modifications and refinements, the solution growth procedure now yields high-quality nanocrystals for a variety of applications. The main advantages of solution growth are:

1. Full control of particle size with high surface area and high purity in comparison with other methods;
2. Particle size can be controlled by adjusting preparation time or by use of a capping agent, and agglomeration is negligible;
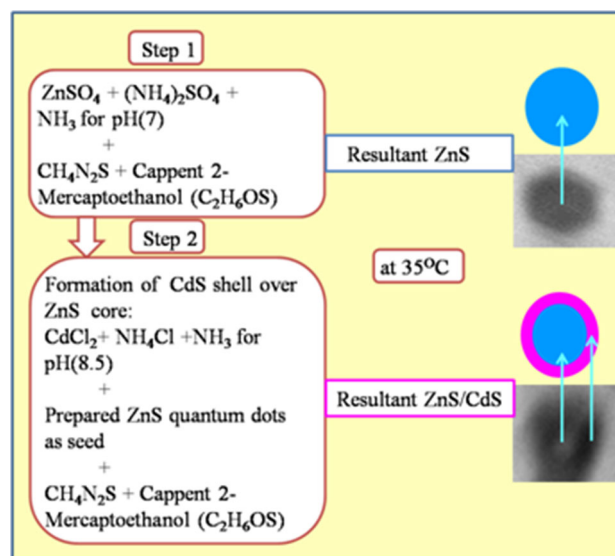

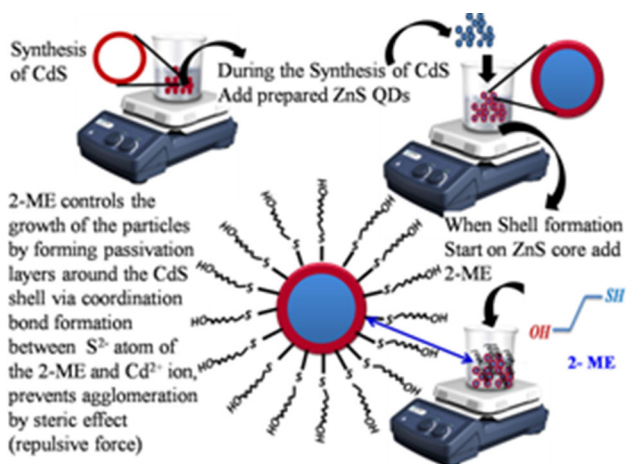Fig. 1. Schematic diagram of the synthesis of ZnS/CdS core/shell QD.

Fig. 2. Schematic diagram of attachment of 2-ME to the CdS shell to control the size of QD by capping.

3. The method requires fewer and inexpensive chemicals;
4. The synthesis is performed at low temperature $(35 \pm 1°C)$;
5. The conditions (thermodynamics and chemistry) used for synthesis of core and shell materials can be readily modified and provide an excellent environment for production of compatible cores and shells;
6. The monodispersed nanoparticles with high luminescence are produced; and
7. ZnS/CdS quantum dots are biocompatible because of use of the capping agent 2-ME.

Characterization Techniques

The optical properties of the QD were studied by use of a Perkin–Elmer (UK) Lambda 2 UV–visible
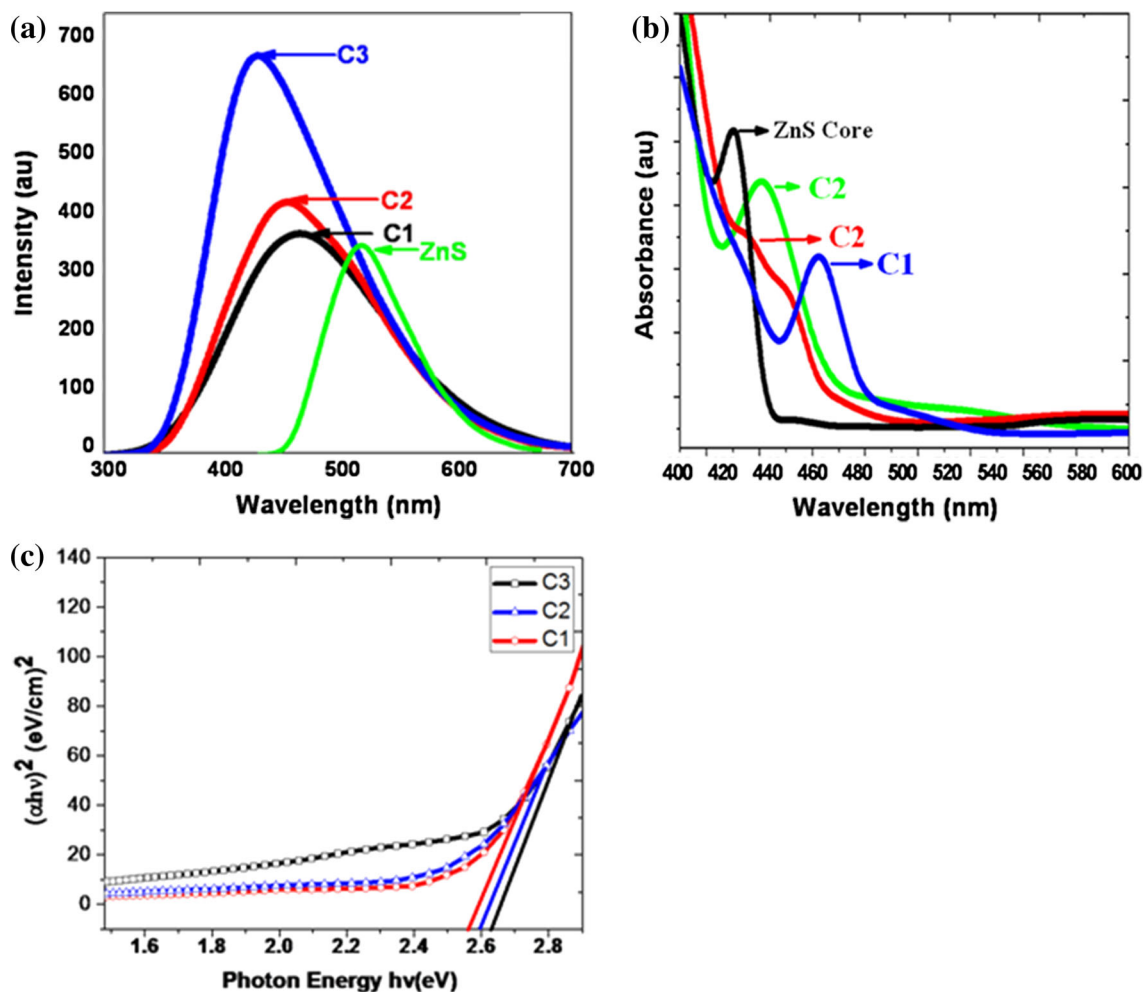

Fig. 3. (a) Photoluminescence spectra of ZnS, C1, C2, and C3 QD; (b) absorption spectra of the ZnS core and C1, C2, and C3 QD; and (c) band gap plot for C1, C2, and C3 QD.

spectrophotometer; absorbance spectra were recorded. Photoluminescence (PL) emission spectra of the samples were recorded by use of a Perkin–Elmer LS55 computer-controlled rationing luminescence spectrophotometer with λ accuracy of ± 1.0 nm and λ reproducibility of ± 0.5 nm. A 20-kW pulse of $< 10 \ \mu$s from a xenon discharge lamp was used as the excitation source for recording photoluminescence emission spectra. A structural investigation was performed by x-ray diffraction (XRD) with a Shimadzu powder x-ray diffractometer using Cu Kα1 radiation. Transmission electron microscopy (TEM; Hitachi H-7500) was performed to determine particle size and particle size distribution. The surface chemistry of the quantum dots was studied by Fourier-transform infrared spectroscopy (FTIR; RZX, Perkin–Elmer).

RESULTS AND DISCUSSION

Mechanism and Effect of the 2-ME

2-ME is water soluble, and is used as a capping molecule and to stabilize the CdS and ZnS/CdS QD. The thiol group acts as the head group and the OH as the tail group. The 2-ME has two functions:

1. It controls the growth of the particles by forming passivation layers around the CdS shell by formation of coordination bonds between the S^{2-} atom of the 2-ME and the Cd^{2+} ion; and/or
2. It prevents agglomeration by steric effects because of repulsion among the OH groups.

The 2-ME thus forms a restricted environment around the CdS QD. The thiol group binds to the Cd ions to the surface of the core/shell QD. Binding of 2-ME with the CdS shell is illustrated in Fig. 2. Binding of capping agents to the nanocrystal surface slows nucleation and growth processes. A longer reaction time enables a more mature nanocrystal growth by Ostwald ripening, which may further change the size and concentration of the nanocrystals. Moreover, the capping agent may create a tightly packed ligand layer on the nanocrystal surface, hindering monomer diffusion to the nanocrystal surface and subsequent reaction. The thiol (–SH) group forms a chelating complex with Cd^{2+}. It is important to mention that the concentration of capping agent in the reaction medium regulates growth of the quantum dots by specific adsorption on different crystal faces.

Luminescence and Absorbance Studies

A wet chemical method was used for synthesis of core and core/shell QD. To obtain a series of inverted ZnS/CdS QD the size of the core was maintained constant and the shell thickness was altered (thus controlling the total size of the shell QD). For convenience, ZnS/CdS QD capped by use of 1 ml, 2 ml and 4 ml 2-ME are denoted C1, C2, and

C3, respectively. It is clear from the PL spectra of C1, C2, and C3 core/shell QD that luminescence intensity decreases with increasing shell thickness (which is in the order C1 > C2 > C3); this effectively enables tuning of PL emission (Fig. 3a).

For C1, for which the shell thickness is maximum, emission intensity is minimum. On reduction of shell thickness to C2 (intermediate shell thickness) then C3 (minimum shell thickness) the PL emission intensity increases but surface defects also increase. This is because of delocalization of the wave functions of electrons and holes in C1 QD, for which the PL spectrum shows emission is maximum at 466 nm. For C2 QD the wave functions of electrons and holes, most probably located in the shell, result in PL emission of maximum intensity at 455 nm. The PL spectrum of C3 is indicative of overlap, which indicates that appropriate shell thickness can enable electron and hole distribution throughout the system. This overlapping and localization of electrons and holes in the core/shell can lead to better PL enhancement and fine tunability; the PL spectrum shows emission is maximum at 430 nm for C3 QD. The PL spectrum of C3 is indicative of approximately twofold enhancement of emission intensity compared with the bare ZnS core, and an overall spectral shift of 70 nm. So, quantum yield can be easily increased by variation of shell (CdS) thickness. For C1 and C2 transitions occur in the shell only, because the thickness is very high; for C3, however, the shell is very thin, so core transitions may have a small effect. A schematic diagram of the functional groups present on the surface of the QD, because of use of the CdS shell and the capping agent (2-ME), and the transitions which can occur, are illustrated in Fig. 4.

This kind of alteration of optical properties is only possible with shells of different sizes. In
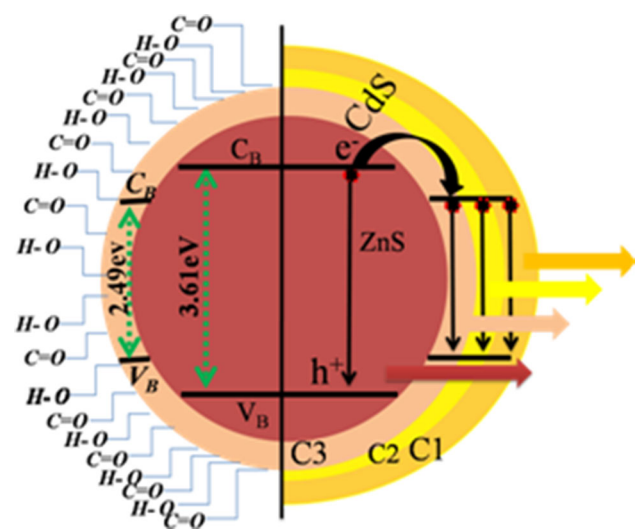

Fig. 4. Schematic diagram of ZnS/CdS inverted core shell QD with CdS layers of different thickness, and possible transitions that can occur in these structures (right). Functional groups present on the surface because of the CdS and 2-ME (left).
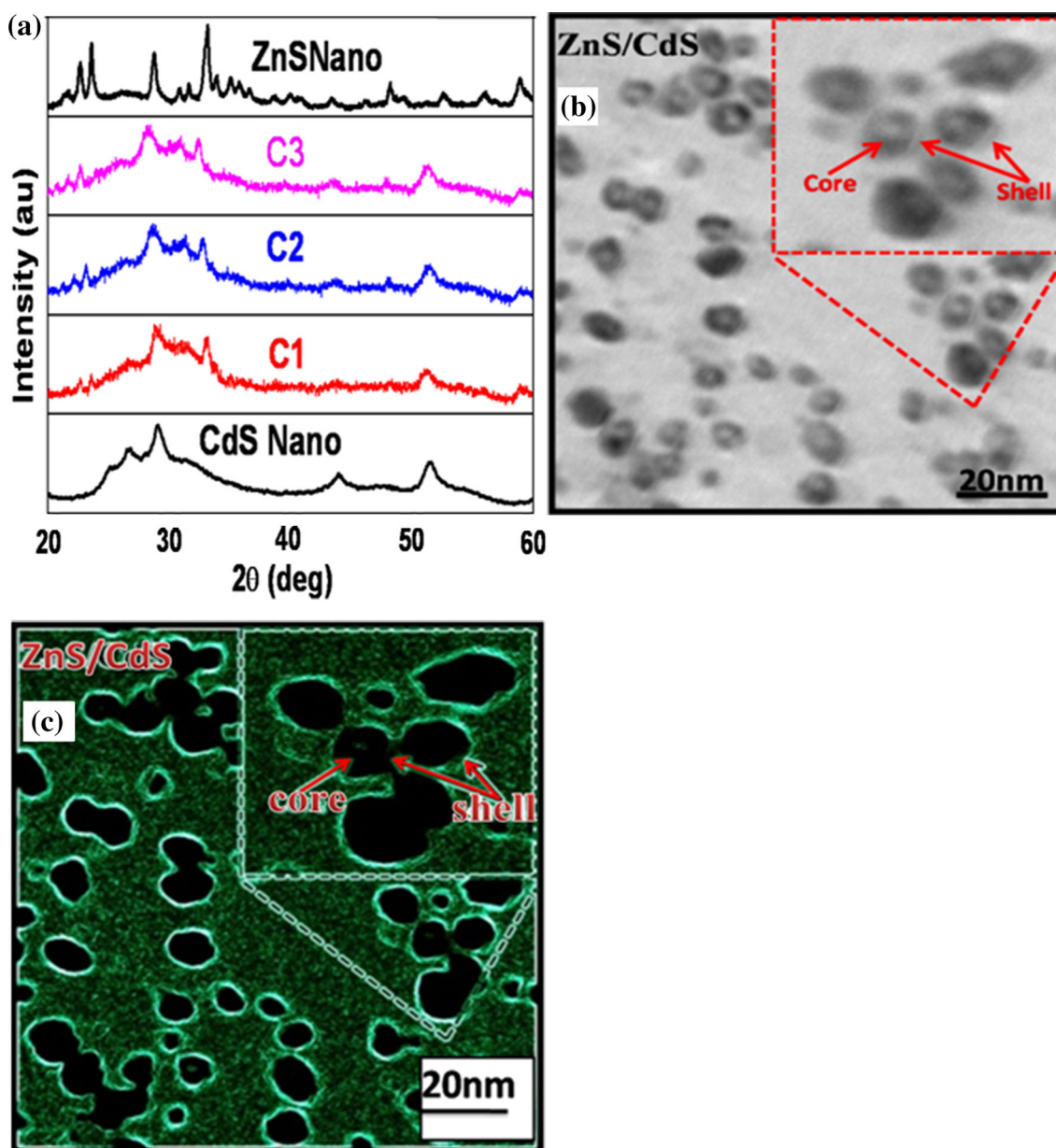
Fig. 5. (a) XRD spectra of CdS, ZnS, C1, C2, and C3 QD; and TEM image of ZnS/CdS (C3) QD (b) before and (c) after processing.

addition, in particular by increasing the thickness of the shell, one can continuously modify carrier location.[17] ZnS/CdS QD prepared by our method are cost-effective, safe, and ecological. The method might also be suitable for synthesis of other inverted core/shell semiconductor QD. The absorption spectra of the 2-ME-capped ZnS core and of C1, C2, and C3 are presented in (Fig. 3b). The absorption edges of the core/shell QD shift toward the red region compared with ZnS QD as QD size is increased, because of the reduced proportion of capping agent. The corresponding band gaps for all the core/shell QD are shown in (Fig. 3c), and were calculated to be 2.58 eV,

2.60 eV, and 2.63 eV for C1, C2 and C3, respectively. This blue shift in absorption onset for C1 to C3 is a clear indication of the quantum confinement effect; the blue shift in absorption onset for ZnS is also indicative of quantum confinement compared with bulk ZnS.[18] The absorption spectrum of C3 contains two shoulders that assumed to originate from radiative recombination of carriers with surface trap states resulting from the combined effect of CdS and the ZnS/CdS interface. With increasing thickness of the shell material, all the coherency stress will be relieved, leading to trapped charge carriers, so the thickness of the shell layer has a critical effect on optical response.

Table I. Structural data for ZnS, ZnS/CdS core/shell (where shell thickness is of the order of C1>C2>C3) and CdS QD (2θ positions, _d_ values, FWHM, intensity, hkl planes, phase assignment, particle size, and lattice constants) and the size of core was kept fixed

Sample	2θ (°)	_d_ (Å) Obs.	_d_ (Å) Stand.	FWHM (°)	Intensity	(hkl)	Phase assignment	Particle size (D) (nm)	Lattice constant (Å)
ZnS (core)	28.68	3.10	3.12	1.34	80	(00,10)	Hexa	3.27	$a = 5.4$ $c = 31.4$
	32.22	2.55	2.66	2.55	25	(107)	Hexa		$a = 3.7$ $c = 30.7$
	58.05	1.56	1.57	1.54	42	(206)	Hexa		$a = 5.4$ $c = 31.2$
C1	29.08	3.06	3.16	2.32	100	(101)	Hexa	5.2	$a = 4.0$ $c = 6.7$
	33.11	2.88	2.90	1.72	40	(200)	Cubic		$a = 3.8$
	51.50	1.72	1.75	1.60	55	(112)	Hexa		$a = 4.0$ $c = 6.5$
C2	29.15	3.06	3.16	2.44	100	(101)	Hexa	4.8	$a = 4.2$ $c = 6.7$
	33.18	2.32	2.90	1.82	40	(200)	Cubic		$a = 3.8$
	51.62	1.71	1.75	1.65	55	(112)	Hexa		$a = 4.1$ $c = 6.7$
C3	29.23	3.06	3.16	2.52	100	(101)	Hexa	4.5	$a = 4.0$ $c = 6.7$
	31.22	2.69	2.90	1.87	40	(200)	Cubic		$a = 3.8$
	51.71	1.45	1.75	1.71	55	(112)	Hexa		$a = 4.1$ $c = 6.7$
CdS QD (for reference)	29.00	3.07	3.16	2.64	100	(101)	Hexa	–	$a = 4.0$ $c = 6.7$
	33.00	2.64	2.90	1.95	40	(200)	Cubic		$a = 3.8$
	51.46	1.77	1.75	1.87	55	(112)	Hexa		$a = 4.0$ $c = 6.5$

Study of Structure and Morphology

For CdS and ZnS QD, selection of precursors and the conditions used for synthesis, especially temperature, is important, because they affect the crystal structure. It has been reported that the precursors $CdCl_2$ and $Cd(NO_3)_2$ give a mixture of cubic and wurtzite phases (Ref. 17 and references therein). XRD patterns were recorded for CdS, C1, C2, C3, and ZnS to check the crystalline phase. It was found that all ZnS/CdS QD could be indexed to the crystalline hexagonal phase of CdS, in agreement with JCPDS-1049 (Fig. 5a). It is worth mentioning that the hexagonal structure is known to be most stable.[19] The 2θ positions, (hkl) planes, and phase assignments corresponding to CdS, C1, C2, C3, and ZnS QD are listed in Table I. The particle size calculated by use of Scherer's formula and lattice constants from XRD data are also listed in Table I. The particle sizes for ZnS and C1, C2, and C3 were 3.27 nm, 5.2 nm, 4.8 nm, and 4.5 nm, respectively.

The particle sizes of the core/shell QD were studied by TEM to confirm the effectiveness of the capping agent and the method of synthesis; the results are presented in Fig. 5a for the smallest QD (C3), with XRD spectrum. Particle size estimated by TEM was 5.5 nm, 5.2 nm, and 4.6 nm for C1, C2 and C3, respectively, slightly higher than the particle sizes obtained from XRD analysis.[19] We further processed the TEM images to make the difference between core (darker area) and shell (bright ring) more visible (Fig. 5c). This is the evidence of the occurrence of two different materials, the ZnS core inside and the CdS shell outside.

Fourier-Transform Infrared Spectroscopy Studies

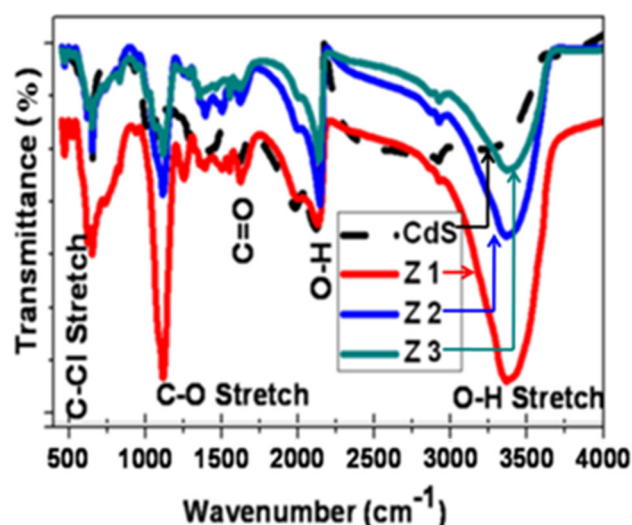The QD were examined by FTIR spectroscopy in the range 4500–400 cm^{-1} (Fig. 6). Broad peaks at

Fig. 6. FTIR spectra of CdS, C1, C2, and C3 quantum dots.

2120 cm^{-1} and 1383 cm^{-1} and a weak peak at 1614 cm^{-1} were assigned to C=C and C–H. A sharp peak at 3365 cm^{-1} was assigned to alcohol O–H and that at 1119 cm^{-1} to amine C–N. Two small peaks at 1626 cm^{-1} were assigned to amine N–H and that at 1401 cm^{-1} to carboxylic acid O–H. OH (hydroxyl), COOH (carboxylic acid), and amine functionality are usually present on biomolecule surfaces,[20,21] and similar functional groups are present on our QD, hence the prepared samples can be easily attached to biomolecules. Because we opted for an aqueous medium for synthesis of the QD, the QD always have hydrophilic surfaces which can be directly attached to biomolecules. This is an additional benefit of our technique; QD prepared by use of high-temperature organic synthesis always acquire hydrophobic surfaces and further surface

processing is needed before bio-conjugation. The synthesized QD are water-soluble and biocompatible, because of the use of 2-ME, and use of the mercapto group to bind to Cd ions on the surface of CdS QD. The carboxyl group on the outer surface of the QD also makes them biocompatible. Because CdS is present on the surface there is a possibility of leaching of Cd into the surrounding medium. To protect the QD from Cd leaching, encasing the QD in either silica or a biocompatible polymer can be advantageous. We, however, are trying to control leaching by binding of the shell by use of a biocompatible thiol group as capping agent.

CONCLUSIONS

A novel low-temperature wet chemical method is proposed for direct growth of type-I inverted hexagonal ZnS/CdS quantum dots (QD). PL spectra of ZnS/CdS QD were red shifted compared with that of the ZnS QD, indicative of the possibility of substantial enhancement of emission by effective tuning. Structural analysis revealed that the ZnS/CdS QD had a hexagonal structure; they were, hence, highly stable. TEM indicated that the average diameter of the QD was 4.6–5.5 nm. The presence of 2-ME on the ZnS/CdS QD was confirmed by FTIR spectroscopy. The proposed mechanism of formation reveals the importance of 2-mercaptoethanol to obtaining stable inverted hexagonal ZnS/CdS QD.

ACKNOWLEDGEMENTS

REFERENCES

1. V.I. Klimov, A.A. Mikhailovsky, S. Xu, A. Malko, J.A. Hollingsworth, C.A. Leatherdale, H.J. Eisler, and M.G. Bawendi, *Science* 290, 314 (2000).
2. V.I. Klimov, eds., *Semiconductor and Metal Nanocrystals: Synthesis and Electronic and Optical Properties* (New York: CRC Press, 2003).
3. B.O. Dabbousi, J.R. Viejo, F.V. Mikulec, J.R. Heine, H. Mattoussi, R. Ober, K.F. Jensen, and M.G. Bawendi, *J. Phys. Chem. B.* 101, 9463 (1997).
4. J. Nanda, S.A. Ivanov, H. Htoon, I. Bezel, A. Piryatinski, S. Tretiak, and V.I. Klimov, *J. Appl. Phys.* 99, 034309 (2006).
5. M.A. Malik, P.O. Brien, and N.A. Revaprasadu, *Chem. Mater.* 14, 2004 (2002).
6. P. Reiss, J. Bleuse, and A. Pron, *Nano Lett.* 2, 781 (2002).
7. M. Danek, K.F. Jense, C.B. Murray, and M.G. Bawendi, *Chem. Mater.* 8, 173 (1996).
8. T. Mokari and U. Banin, *Chem. Mater.* 15, 3955 (2003).
9. M. Ethayaraja, C.R. Kumar, D. Muthukumaran, K. Dutta, and R.J. Bandyopadhyaya, *Phys. Chem. C* 111, 3246 (2007).
10. S.A. Ivanov, J. Nanda, A. Piryatinski, M. Achermann, L.P. Balet, I.V. Bezel, P.O. Anikeeva, S. Tretiak, and V.I. Klimov, *J. Phys. Chem. B.* 108, 10625 (2004).
11. M. Koneswaran and R. Narayanaswamy, *Microchim. Acta* 178, 171 (2012).
12. J.G. Díaz, M. Zieliński, W. Jaskólski, and G.W. Bryant, *Phys. Rev. B* 74, 205309 (2006).
13. J. Pérez-Conde and A.K. Bhattacharjee, *Phys. Rev. B* 67, 235303 (2003).
14. N. Soltani, E. Saion, M. Erfani, A. Bahrami, M. Navaseri, K. Rezaee, and M.Z. Hussein, *Chalcogenide Lett.* 9, 379 (2012).
15. M. Sharma, D. Gupta, D. Kaushik, A.B. Sharma, and R.K. Pandey, *J. Nanosci. Nanotechnol.* 8, 1 (2008).
16. G. Faming, *Appl. Phys. Lett.* 98, 193105 (2011).
17. H. Kumar, M. Kumar, P.B. Barman, and R.R. Singh, *Appl. Phys. A* 117, 1249 (2014).
18. S. Kim, B. Fisher, H.J. Eisler, and M.G. Bawendi, *J. Am. Chem. Soc.* 125, 11466 (2003).
19. E.R. Goldman, E.D. Balighia, H. Mattoussi, M.J. Kuno, M. Mauro, and P.T. Tran, Anderson GP. *J. Am. Chem. Soc.* 124, 6378 (2002).
20. M. Bruchez Jr, M. Moronne, P. Gin, S. Weiss, and A.P. Alivisatos, *Science* 281, 2013 (1998).
21. J. Archana, M. Sabarinathan, M. Navaneethan, S. Ponnusamy, and C. Muthamizhchelvan, Hayakawa. *Mater. Lett.* 125, 35 (2014).